J Nanostruct Chem (2015) 5:7–15
DOI 10.1007/s40097-014-0123-0

ORIGINAL

Synthesis, characterization, and application of Nd, Zr–TiO_2/SiO_2 nanocomposite thin films as visible light active photocatalyst

Susan Samadi · Mohammad Yousefi ·
Faezeh Khalilian · Ameneh Tabatabaee

Received: 22 May 2014 / Accepted: 26 August 2014 / Published online: 2 October 2014

Abstract A novel Nd, Zr–TiO_2/SiO_2 nanocomposite thin film was successfully prepared with various amounts of Nd^{3+} and Zr^{4+} as codopant ions for self-cleaning applications. In the first step, two types of Zr, Nd–TiO_2/SiO_2 thin films were prepared using $ZrCl_4$ and $ZrOCl_2$ compounds as a source of second doping agent ions. The result of the scanning electron microscopy (SEM) indicated that $ZrOCl_2$ precursor produces a more monotonous thin film, but study of the photocatalytic activity of these thin films showed that $ZrCl_4$-based thin film possess a more significant photocatalytic activity. Based on these results, $ZrCl_4$ was chosen as a source of doping ion. Two kinds of Nd, Zr–TiO_2/SiO_2 nanocomposite thin films A and B were synthesized using various techniques. Type A thin film was coated on a glass substrate by heat treatment, but Type B was coated on polycarbonate sheets without any heat treatment process. The SEM images and XRD pattern showed that the optimum amount of doping ion in relation to Ti^{3+} is 0.1 %. In this circumstance, the most monotony of film was seen and the main formed phase was anatase. The sample structures were characterized by infrared spectroscopy. The nanocomposite films were found to be active for photocatalytic decomposition of methyl orange as an organic pollutant.

Keywords Codoped TiO_2 · Photocatalytic application · Self-cleaning · Visible light

S. Samadi (✉) · M. Yousefi · F. Khalilian · A. Tabatabaee
Department of Chemistry, College of Basic Science,
Yadegar-e-Imam Khomeini (RAH) Branch, Islamic Azad
University, Tehran, Iran
e-mail: susansamadi@iausr.ac.ir; s.samadi2008@yahoo.com

Background

Nanocomposites have been a topic of intense research mainly because of their unique physical and chemical properties. Titania in particular has recently attracted so much interest owing to their potentials for revolutionary photocatalytic applications, optical properties, photovoltaic cells and gas sensors [1–6]. However, titania has relatively high band gap energy (3.2 eV) which limits its applications in visible light range of electromagnetic spectrum [7].

Efficiency of electron–hole separation is important for photocatalytic applications and optical properties. Furthermore, titania photocatalytic activity has been improved by doping with transition metal impurities. These doping agents trap charge carriers and decrease the electron–hole recombination and increase production of OH° in the photocatalytic activity [8–14]. The effect of doping on the photocatalytic activity depends on several factors such as ion types, concentration of ions and the method of ion doping [15]. Different positions of the dopant in the host lattice cause various influences on trapping electrons and/or holes on the surface or during interface charge transfer [16].

To enhance the photocatalytic activity under visible light, effect of different metals [16] and nonmetals [17] has been widely studied. During last decades, codoped ions have been used to increase the photocatalytic activity of TiO_2 under both UV and visible light. S–N-codoped TiO_2 [18], F–N-codoped TiO_2 [19], B–N-codoped TiO_2 [20] and C–N-codoped TiO_2 powder [21] were used to enhance the photocatalytic efficiency under visible light and prevent the reduction of photocatalytic activity as a result of charge recombination. During last decade, there are some reports on using Nd [7, 16, 22, 23] and Zr [24, 25] ions as dopant in TiO_2 nanoparticles to enhance photocatalytic degradation of some organic pollutants and heavy metals.

Table 1 Formulation of sample thin films

No. of samples	Samples content	Amount of Nd^{3+} (molar ration vs. Ti^{4+})	Amount of Zr^{4+} (molar ration vs. Ti^{4+})
S_1	TiO_2/SiO_2	–	–
S_2	Nd–TiO_2/SiO_2	0.2 %	–
S_3	Nd, Zr–TiO_2/SiO_2	0.15 %	0.05 %
S_4	Nd, Zr–TiO_2/SiO_2	0.1 %	0.1 %
S_5	Nd, Zr–TiO_2/SiO_2	0.05 %	0.15 %
S_6	Zr–TiO_2/SiO_2	–	0.2 %

It is becoming increasingly difficult to ignore the kind of TiO_2 phase on the photocatalytic activity. It is well known that the best form is anatase phase for photocatalytic degradation. Among the different phases of TiO_2, anatase/rutile interface shows more activity because of reducing the recombination of photogenerated electrons and holes [26].

Previous researches indicate that the addition of SiO_2 and dispersive agent to TiO_2 films creates an extremely large surface and increases photoinduced super hydrophilicity [27, 28].

In this study, the effect of Nd^{3+} and Zr^{4+} ions as codopants in TiO_2/SiO_2 nanocomposite thin film on glass and poly carbonate sheet (PC) was investigated. As precursor ion doped has influence on photocatalytic activity, two precursors of $ZrCl_4$ and $ZrOCl_2$ were chosen as a source of Zr^{4+} dopant. Two types of nanocomposites were

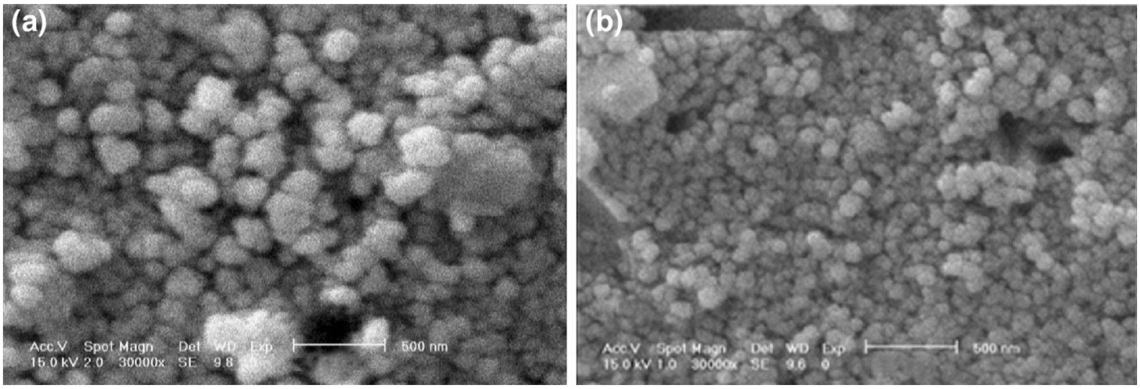

Fig. 1 The SEM images of two types of Zr, Nd–TiO_2/SiO_2 thin films: **a** $ZrCl_4$, **b** $ZrOCl_2$ as a source of second doping agent ions

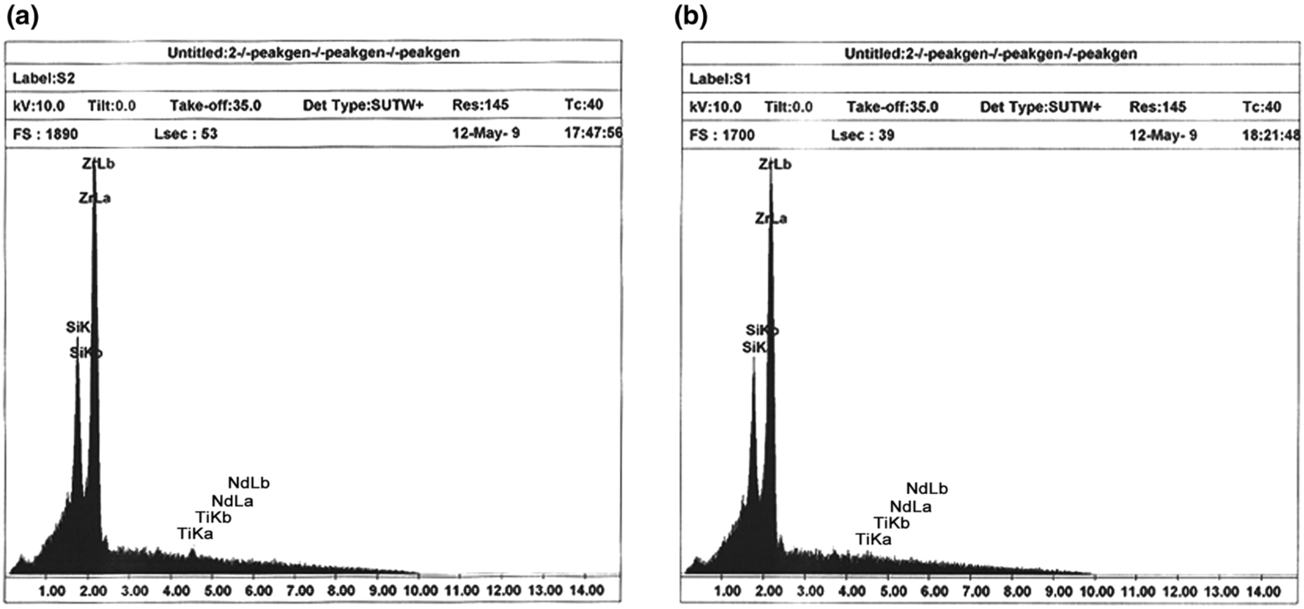

Fig. 2 The EDX analysis of two types of Zr, Nd–TiO_2/SiO_2 thin films: **a** $ZrCl_4$, **b** $ZrOCl_2$ as a source of second doping agent ions

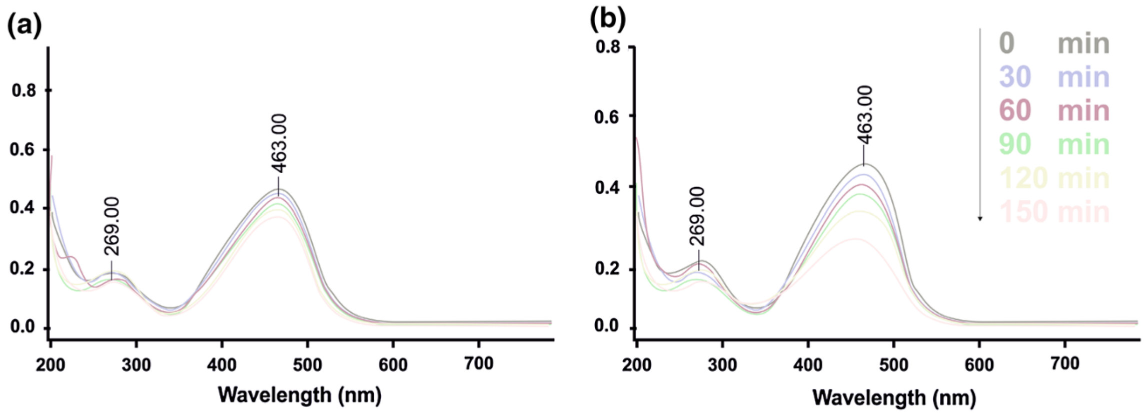

Fig. 3 Photodegradation rate of methyl orange solution under visible light irradiation condition: **a** $ZrOCl_2$, **b** $ZrCl_4$ as a source of second doping agent ions

synthesized. By comparing microstructure and photocatalytic activity, the most suitable precursor was selected.

Methods

Materials

Titanium tetra isopropoxide (TTIP), Zirconium (IV) Chloride and Neodymium (III) acetate (AR analytical grade, Merck Chemical Company) were used as Titanium, Zr^{4+} and Nd^{3+} sources for the synthesis of Zr, Nd–TiO_2 nanocomposite. Hydroxy Propyl Cellulose (HPC) was used as dispersion; HNO_3, SiO_2 colloid solution (Ludox) and absolute ethanol were purchased from Merck Chemical Company. Double distilled water was used in all of the experiments.

Photocatalysis and characterizations

SEM-XL30 scanning electron microscope was used to determine the microstructure of the thin film samples, while it was coated by gold. EDX analysis was performed by SEM-XL30 and D-500 spectroscopy (Siemens). X-Ray powder diffraction data were collected on SCIFERT-3003 PTS. FT-IR spectra were obtained using a Thermo Nicolet NEXUS-870. The photocatalytic degradation of methyl orange dilute solution was performed by measuring optical absorption at the 465 nm wavelength before and after the illumination of visible range of electromagnetic radiation by Varian UV–Vis Spectrophotometer. In Photocatalytic experiments, light source was 400 W high-pressure mercury vapor lamp (Osram).

The solution of methyl orange in deionized water with a concentration of 5 ppm was chosen as a matter of photodegradation. This solution was set in the vicinity of thin film samples under visible light irradiation. The spectrum

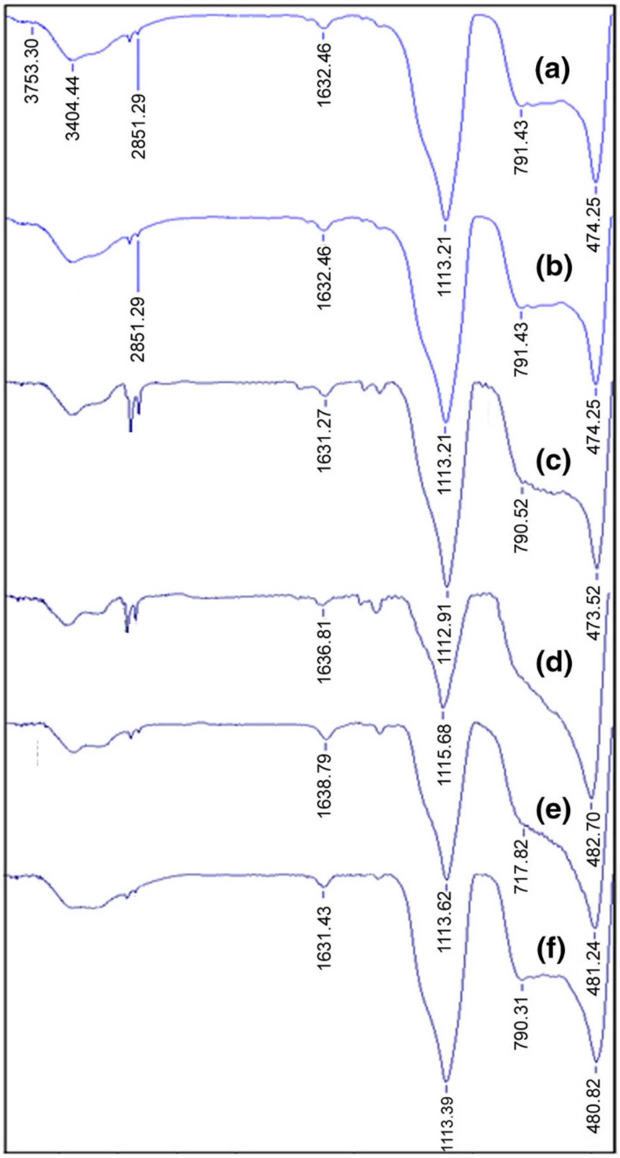

Fig. 4 The FT-IR spectra of the sol–gel nanocomposites: **a** sample 1, **b** sample 2, **c** sample 3, **d** sample 4, **e** sample 5 and **f** sample 6

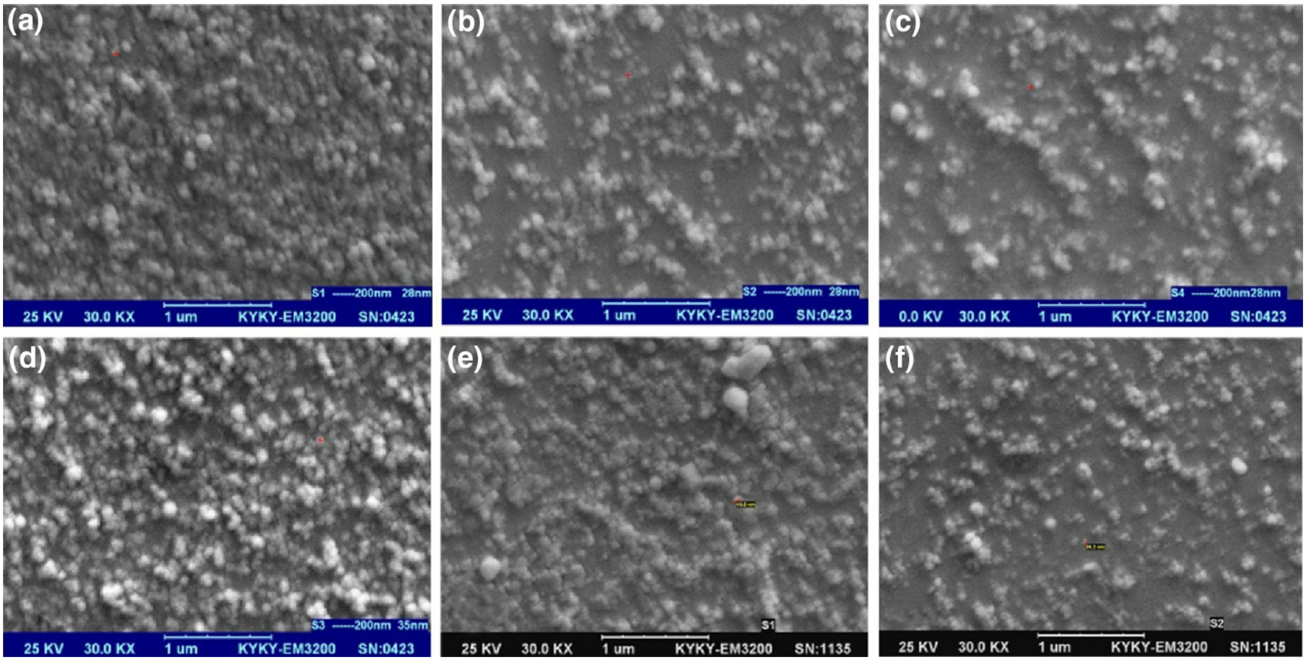

Fig. 5 SEM images for the sample films: **a** sample 1, **b** sample 2, **c** sample 3, **d** sample 4, **e** sample 5 and **f** sample 6

of Osram HQL (MBF-U) 400W-E40 lamp was reported by Azar et al. [29].

Preparation of samples

Two types of Zr, Nd–TiO_2/SiO_2 thin films were prepared based on using $ZrCl_4$ and $ZrOCl_2$ compounds as a source of second doping agent ions.

In addition, two kinds of sample solutions A and B were prepared. The preparation of sample solution A is described in details elsewhere [29, 30]. First, TTIP was dissolved in absolute ethanol. Then, this dispersed solution was added with molar ratio TTIP:C_2H_5OH:dispersion equals to 1:125:4.5 × 10^{-3} $gg_{sol.}^{-1}$ and stirring until complete dissolution. Afterwards, the mixture of C_2H_5OH, HNO_3, water, and SiO_2 with molar ratio of ethanol:HNO_3:H_2O:SiO_2 equals to 43:0.2:1:0.30 and various amounts of $Nd(CH_3COO)_3$ and $ZrCl_4$ (refer to Table 1) were added dropwise under vigorous stirring. The obtained colloidal suspension was transparent and stirred for 45 min and then aged for 48 h until gel formed.

The solution B was prepared based on a reported method by Yaghobi et al. [31], and the only difference was the addition of SiO_2 colloidal solution, Nd^{3+} and Zr^{4+} as doping ions. H_2O was added to H_2O_2, with volume proportions of 90:200, respectively (solution 1). Nd^{3+}, Zr^{4+} with 0.001 molar ratios vs. TiO_2, SiO_2 and HPC was dissolved in absolute ethanol (solution 2). Then, solution 2 was added dropwise to solution 1 with vigorous stirring (solution 3). Following, 12 ml TTIP was added to solution 3 dropwise for 30 min with vigorous stirring. NaOH was added to the solution to raise pH to 7. Finally, the obtained solution was refluxed for 10 h to form anatase sol.

The glass substrates and polycarbonate sheets were washed first by detergent and water, in order and they were rinsed with deionized water. These sheets were more cleaned by 2-propanol and then acetone ultrasonically and were rinsed again with water and then were dried. The surface of PC sheets was made by adding dropwise of 37.5 ml H_2SO_4 to 4 g $K_2Cr_2O_7$ and then by the addition of 12.5 ml water. Cooling the solution to room temperature, the PC sheets were sunk in the solution for 17 min.

Sample layers were coated on glasses and PC substrates using dip coating at 3 mm/s. For PC substrates, the peroxotitanium complex solution was used as a pre-coat and applied initially on the surface of PC substrates to increase the adhesion and acts as a barrier for photocatalytic reaction on PC.

Afterwards, the glass substrates were coated by sample solutions A, with dip-coating method. Finally, the porous nanocomposite films were obtained after heat treatment for 2 h at 500 °C in air.

Subsequently, the crystalline TiO_2 layers were deposited on the PC sheets by three times dip coating with sample solution B. Consequently, the resulting sample was dried in a furnace at 90 °C for 1 h.

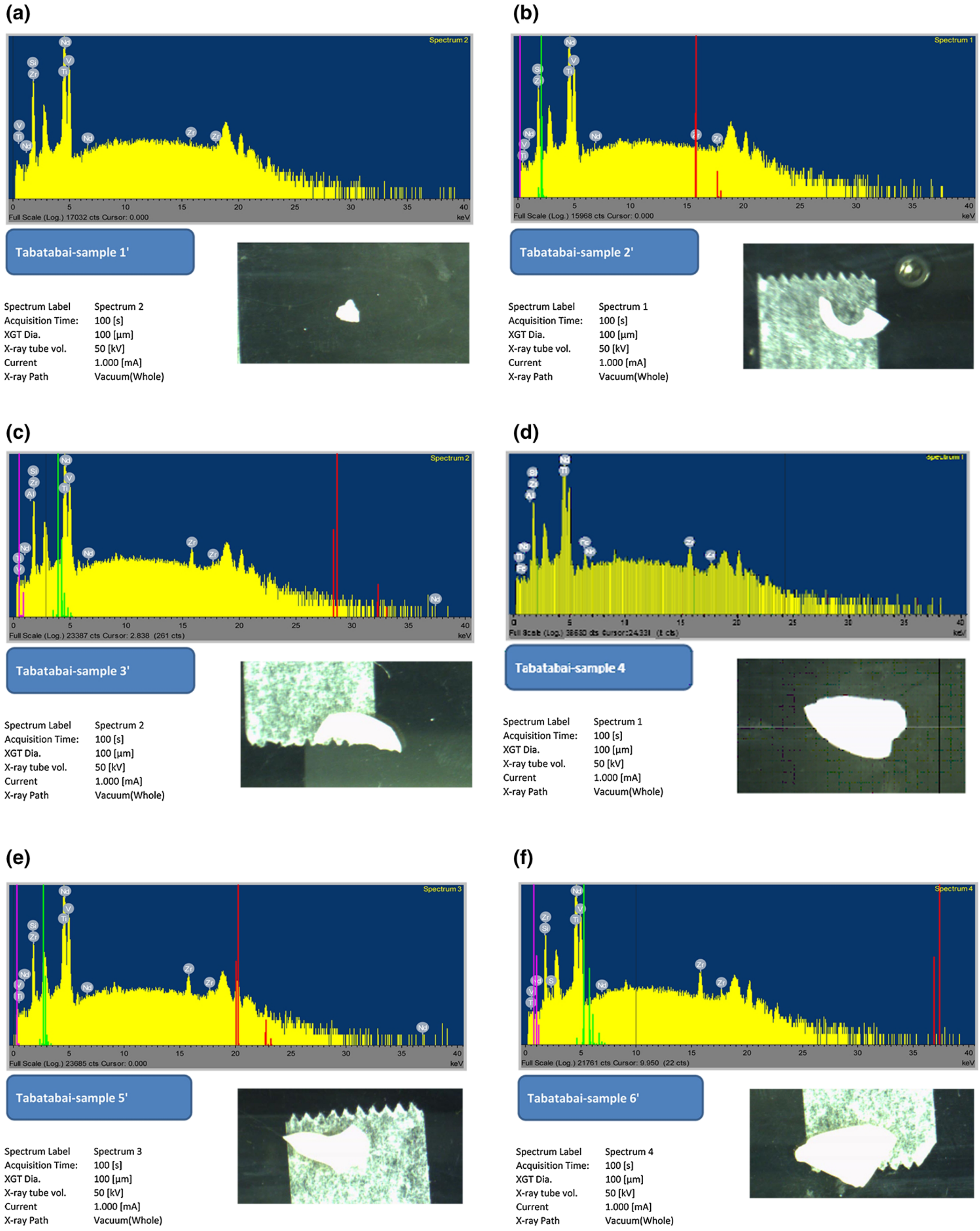

(a)

Spectrum Label	Spectrum 2
Acquisition Time:	100 [s]
XGT Dia.	100 [μm]
X-ray tube vol.	50 [kV]
Current	1.000 [mA]
X-ray Path	Vacuum(Whole)

(b)

Spectrum Label	Spectrum 1
Acquisition Time:	100 [s]
XGT Dia.	100 [μm]
X-ray tube vol.	50 [kV]
Current	1.000 [mA]
X-ray Path	Vacuum(Whole)

(c)

Spectrum Label	Spectrum 2
Acquisition Time:	100 [s]
XGT Dia.	100 [μm]
X-ray tube vol.	50 [kV]
Current	1.000 [mA]
X-ray Path	Vacuum(Whole)

(d)

Spectrum Label	Spectrum 1
Acquisition Time:	100 [s]
XGT Dia.	100 [μm]
X-ray tube vol.	50 [kV]
Current	1.000 [mA]
X-ray Path	Vacuum(Whole)

(e)

Spectrum Label	Spectrum 3
Acquisition Time:	100 [s]
XGT Dia.	100 [μm]
X-ray tube vol.	50 [kV]
Current	1.000 [mA]
X-ray Path	Vacuum(Whole)

(f)

Spectrum Label	Spectrum 4
Acquisition Time:	100 [s]
XGT Dia.	100 [μm]
X-ray tube vol.	50 [kV]
Current	1.000 [mA]
X-ray Path	Vacuum(Whole)

Fig. 6 The EDX analysis of two types of Zr, Nd–TiO_2/SiO_2 thin films: **a** sample 1, **b** sample 2, **c** sample 3, **d** sample 4, **e** sample 5 and **f** sample 6

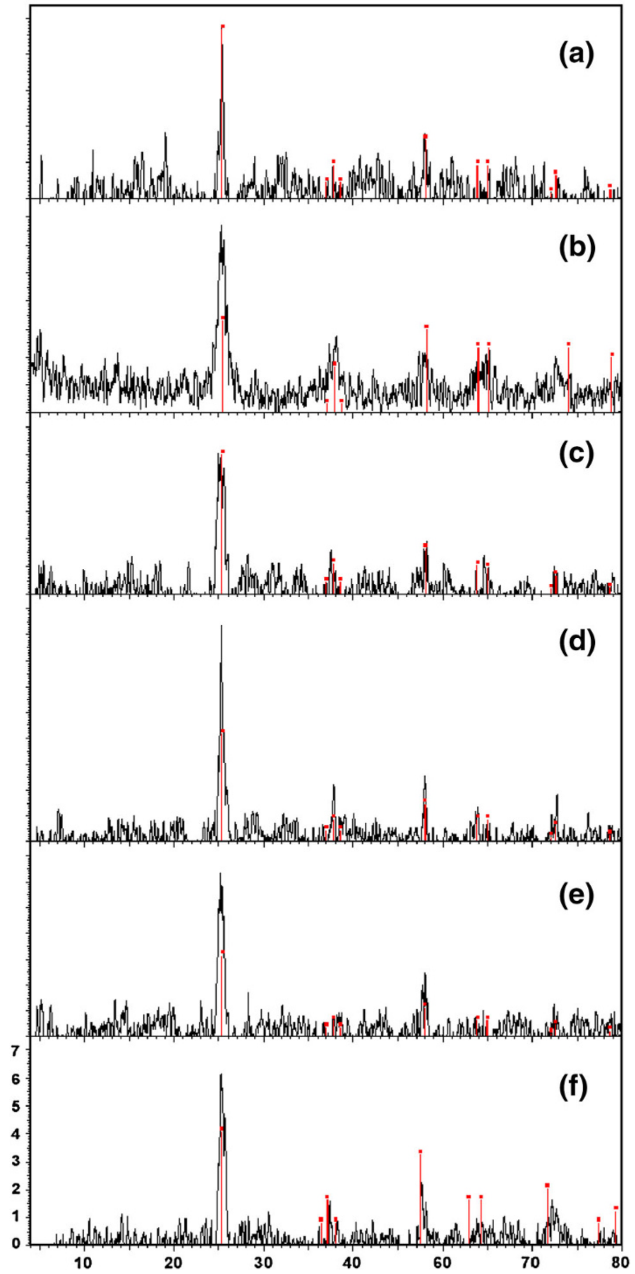

Fig. 7 XRD patterns of sol–gel synthesized nanocomposites: **a** sample 1, **b** sample 2, **c** sample 3, **d** sample 4, **e** sample 5 and **f** sample 6

Results and discussion

The effect of zirconium precursor

The SEM images of two types of Nd, Zr–TiO_2/SiO_2 nanocomposite thin films are presented in Fig. 1. As displayed, $ZrOCl_2$ precursor resulted in a more monotonous thin film. The EDX analysis illustrated in Fig. 2 represents the presence of Zr and Nd as doping ions.

The photocatalytic activity of these thin films was investigated as well. According to Fig. 3, $ZrCl_4$-based thin film possesses a more significant photocatalytic activity; and the microstructure of this film became loose. Based on these results, $ZrCl_4$ was chosen as a source of doping ion.

The effect of Zr^{4+} and Nd^{3+} on the microstructure

FT-IR spectra of the samples with different amounts of Zr^{4+} and Nd^{3+} are shown in Fig. 4. The stretching bands at 2,060–3,600 cm^{-1} are assigned to symmetric vibration of surface hydroxyl group [7, 32, 33]. The strong band at 3,100–3,700 cm^{-1} is attributed to hydroxyl group that is obtained from TTIP hydrolysis. The strong bands at about 1,630 cm^{-1} have been assigned to H–OH bending vibration of physically adsorbed water and hydroxyl group [7]. The band at 791 cm^{-1}, along with a weak band at 960 cm^{-1} are commonly assigned to vibration of Si–O–Ti band [34]. The bands around 1,113 cm^{-1} can be related to asymmetric stretching of the Ti–O bands [35, 36]. Consequently, the presence of these bands confirms the existence of Si–O–Ti bands in the Nd–TiO_2/SiO_2 nanocomposite. Similarly as in the other Ti–Nd composites, the peak at 470 cm^{-1} is attributed to the anatase skeletal O–Ti–O–Nd linkages [37, 38].

The SEM images are illustrated in Fig. 5. Having Zr^{4+} and Nd^{3+} metal ions or the mixture of them on the thin film would have influence on particle size. When Zr^{4+} metal ion was added to nanocomposite, monotonous of film was decreased. In sample 4 that molar ratio of doping ions is 0.1 % vs. Ti^{3+}, nanocomposite particle size was decreased and distribution was come narrow and coating was monotonously without any agglomeration. The analysis of EDX is shown in Fig. 6 in the presence of Zr and Nd as doping ions.

The effects of Zr^{4+} and Nd^{3+} on the anatase phase

The XRD patterns of S_1, S_2, S_3, S_4, S_5 and S_6 are shown in Fig. 7a–g. The unique peaks at $2\theta = 25.5°$ and 38.1° are assigned to the anatase crystal. There is no evidence of mixed rutile and anatase phases and only anatase structure is observed.

According to the Fig. 7, proportions of anatase phase in the samples were different and the sample 4 was crystalline and has only anatase form. As reported, the crystalline phase possesses a key role in photocatalytic activity of organic compounds in a way that the rutile phase is much less active [7].

As expected, the sample 4 was the best candidate for self-cleaning activity. It might be concluded that at 500 °C,

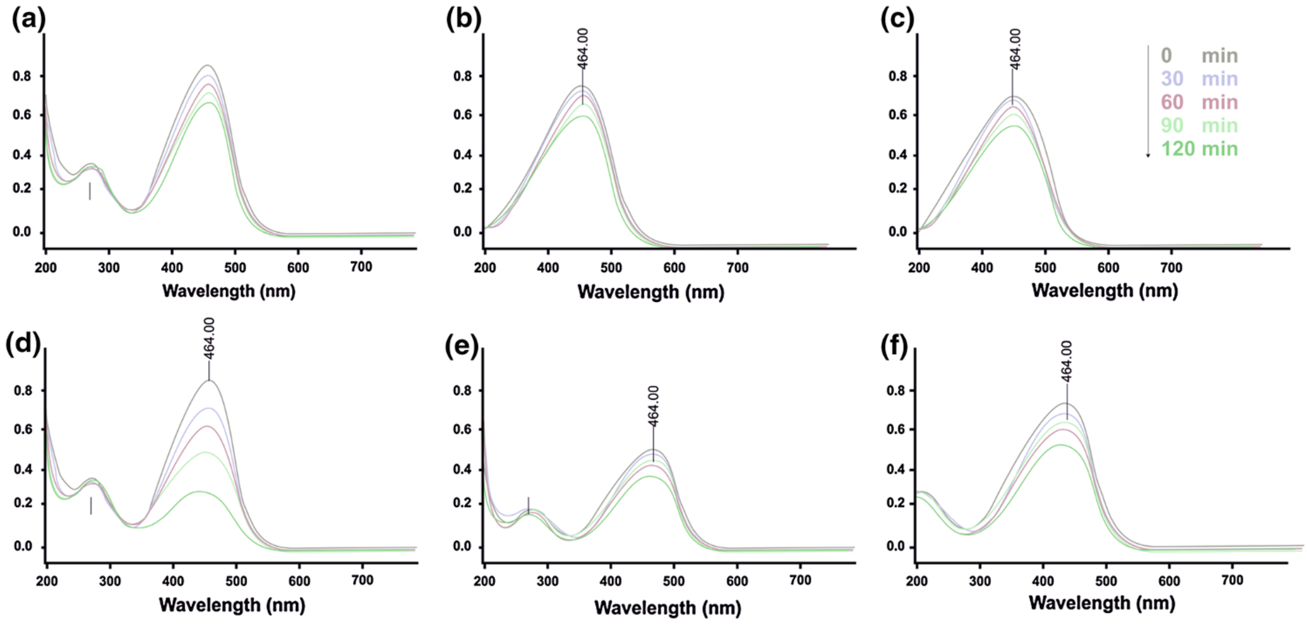

Fig. 8 Photodegradation rate of methyl orange solution under visible light irradiation: **a** sample 1, **b** sample 2, **c** sample 3, **d** sample 4, **e** sample 5 and **f** sample 6

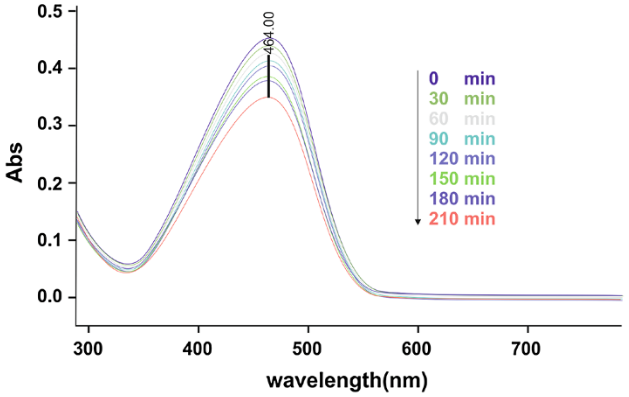

Fig. 9 Photodegradation rate of methyl orange solution under visible light irradiation with $Nd_{0.1\ \%}$, $Zr_{0.1\ \%}$–TiO_2/SiO_2 nanocomposite thin films on PC sheets

the addition of Nd^{3+} and Zr^{4+} has facilitated the formation of anatase phase.

The effects of Zr^{4+} and Nd^{3+} on the self-cleaning ability

Figure 8 shows the relationship between the amount of Zr^{4+} and Nd^{3+} metal ions on photocatalytic activity of the samples. It is found that the photocatalytic activity would be improved by addition of Zr^{4+} to Nd^{3+} as a second doping ion. The decomposition time of methyl orange, in electromagnetic visible light range, would be reduced, when molar ratio of Zr^{4+} and Nd^{3+} was 0.1 % vs. Ti^{3+}.

The amount of Zr^{4+} or Nd^{3+} is one of the most important parameter in photocatalytic degradation since these changes have a severe effect on the microstructure of the films. By addition of certain amount of Zr^{4+} to Nd^{3+}, the Nd, Zr–TiO_2/SiO_2 obtained porous films and decreased particle size in the suitable condition. As a result, the adequate self-cleaning activity of sample 4 under visible light would be attributed to the spongy microstructure.

The photocatalytic effect of film on the PC sheets was studied as well. Figure 9 shows degradation of methyl orange solution by thin film of solution B without any heat treatment which is a usual process after sol–gel method. In this method of synthesis, reflux process was formed anatase phase in titania. The reduced concentration of methyl orange solution confirmed the formation of anatase phase and photocatalytic activity of nanocompostite film on the PC sheets.

Conclusions

The six types of TiO_2/SiO_2 photocatalyst thin films including various amounts of Nd^{3+} and Zr^{4+} were synthesized by sol–gel method. The results indicate that addition of Nd^{3+} and Zr^{4+} as a codopant has influence on distribution and monotonous coating of TiO_2/SiO_2 thin film. The amount of codopant dictates the distribution of Nd–TiO_2/SiO_2 films. $Nd_{0.1\ \%}$, $Zr_{0.1\ \%}$–TiO_2/SiO_2

nanocomposite thin films have the best uniform particle distribution among samples with low agglomeration, spongy microstructure and photocatalytic activity.

Acknowledgments The authors gratefully acknowledge the financial and other supports of this research, provided by the Islamic Azad University, Yadegar-e-Imam Khomeini (RAH) Branch, Tehran, Iran.

References

1. Raut, N.C., Mathews, T., Chandramohan, P., Srinivasan, M.P., Dash, S., Tyagi, A.K.: Effect of temperature on the growth of TiO_2 thin films synthesized by spray pyrolysis: structural, compositional and optical properties. Mater. Res. Bull. **46**, 2057–2063 (2011)
2. Piispanen, M., Hupa, L.: Comparison of self-cleaning properties of three titania coatings on float glass. Appl. Surf. Sci. **258**, 1126–1131 (2011)
3. Liu, Z., Misra, M.: Dye-sensitized photovoltaic wires using highly ordered TiO_2 nanotube arrays. ACS Nano **4**, 2196–2200 (2010)
4. Hsiao, P.T., Tung, Y.L., Teng, H.: Electron transport patterns in TiO_2 nanocrystalline films of dye-sensitized solar cells. J. Phys. Chem. C **114**, 6762–6769 (2010)
5. Sanchez, M., Rincom, M.E., Guirado-Lopez, R.A.: Anomalous sensor response of TiO_2 films: electrochemical impedance spectroscopy and ab initio studies. J. Phys. Chem. C **113**, 21635–21641 (2009)
6. Moon, H.G., Shim, Y.S., Jang, H.W., Kim, J.S., Choik, J., Kang, C.Y., Choi, H.H., Yoon, S.: Highly sensitive CO sensors based on cross-linked TiO_2 hollow hemispheres. J. Sens. Actuators B Chem. **149**, 116–121 (2010)
7. Parida, K.M., Sahu, N.J.: Visible light induced photocatalytic activity of rare earth titania nanocomposites. Mol. Catal. A Chem. **287**, 151–158 (2008)
8. Zalas, M., Laniecki, M.: Photocatalytic hydrogen generation over lanthanides-doped titania. Sol. Energy Mater. Sol. Cells **89**, 287–296 (2005)
9. Xie, Y., Yuan, C., Li, X.: Photocatalytic degradation of X-38 dye by visible light using lanthanide ion modified titanium dioxide hydrosol system. Colloids Surf. A **252**, 87–94 (2005)
10. Yan, X., He, J., Evans, D., Duran, X., Zhu, Y.: Preparation, characterization and photocatalytic activity of Si-doped and rare earth-doped TiO_2 from mesoporous precursors. Appl. Catal. B Environ. **55**, 243–252 (2005)
11. Cuiying, H., Wansheng, Y., Liqin, D., Zhibin, L., Zhengang, S., Lancui, Z., Chin, J.: Effect of Nd^{3+} doping on photocatalytic activity of TiO_2 nanoparticles for water decomposition to hydrogen. Catalyst **27**, 203–209 (2006)
12. Peng, T., Zhao, D., Song, H., Yan, C.: Preparation of lanthana-doped titania nanoparticles with anatase mesoporous walls and high photocatalytic activity. J. Mol. Catal. A: Chem. **238**, 119–126 (2005)
13. Miljevic, M., Geiseler, B., Bergfeldt, Th, Bockstaller, P., Fruk, L.: Enhanced photocatalytic activity of Au/TiO_2 nanocomposite prepared using bifunctional bridging linker. Adv. Mater. **24**, 907–915 (2014)
14. Li, F., Li, X., Hou, M.: Significant effect of lanthanide doping on the texture and properties of nanocrystalline mesoporous TiO_2. Appl. Catal. B Environ. **48**, 185–194 (2004)
15. Azar, P.A., Dehaghi, S.M., Samadi, S., Kamyar, S., Saber Tehrani, M.: Effect of Nd^{3+}, pectin and poly (ethylene glycol) on the photocatalytic activity of TiO_2/SiO_2 film. Asian J. Chem. **22**, 1619–1627 (2010)
16. Shah, S.I., Li, W., Huage, H.P., Jung, O., Ni, C.: Study of Nd^{3+}, Pd^{2+}, Pt^{4+}, and Fe^{3+} sopant effect on photoreactivity of TiO_2 nanoparticles. PANS **99**, 6482–6486 (2002)
17. Xu, Q.C., Wellia, D.V., Sk, M.A., Lim, K.H., Chye, S.C.J., Liao, D.W., Amal, R., Tan, T.T.Y.: Transparent visible light activated C–N–F-codoped TiO_2 films for self-cleaning application. J. Photoch. Photobiol. A **210**, 181–187 (2010)
18. Xu, J.H., Li, J., Dai, W.L., Cao, Y., Li, H., Fan, K.: Simple fabrication of twist-like helix N, S-codoped titania photocatalyst with visible-light response. Appl. Catal. B Environ. **79**, 72–80 (2008)
19. Li, D., Haneda, H., Hishita, S., Ohashi, N.: Visible-light-driven N-F-codoped TiO_2 photocatalysts 1. Synthesis by spray pyrolysis and surface characterization. Chem. Mater. **17**, 2588–2595 (2005)
20. Liu, G., Zhao, Y., Sun, C., Li, F., Lu, G.Q., Cheng, H.M.: Sinergistic effects of B/N doping on the visible-light photocatalytic activity of mesoporous TiO_2. Angew. Chem. Int. Ed. **47**, 128–133 (2008)
21. Yang, X., Cao, C., Erikson, L., Hohn, L., Magirang, R., Klabund, K.: Synthesis of visible-light-active TiO_2-based photocatalysts by carbon and nitrogen doping. J. Catal. **260**, 128–133 (2008)
22. Burns, A., Li, W., Baker, C., Shah, S.I.: Sol–gel synthesis and characterization of neodymium-ion doped nanostructured titania thin films. Mat. Res. Soc. Symp. Proc. **703** V5.2.1–V.5.2.6 (2002)
23. Rengaraj, S., Venkataraj, S., Yeon, J.W., Kim, Y., Li, X.Z., Pang, G.K.H.: Preparation, characterization and application of Nd-TiO_2 photocatalyst for the reduction of Cr(VI) under UV light illumination. Appl. Catal. B Environ. **77**, 157–165 (2007)
24. Chang, S.M., Doong, R.A.: Characterization of Zr-doped TiO_2 nanocrystals prepared by a nonhydrolytic sol–gel method at high temperatures. J. Phys. Chem. B **110**, 20808–20814 (2006)
25. Gao, B., Lim, T.M., Subagio, D.P., Lim, T.T.: Zr-doped TiO_2 for enhanced photocataytic degradation of bisphenol A. Appl. Catal. A Gen. **375**, 107–115 (2010)
26. Yan, M., Chen, F., Zhang, J., Anpo, M.: Preparation of controllable crystalline titania and study on the photocatalytic properties. J. Phys. Chem. B **109**, 8673–8678 (2005)
27. Guan, K., Lu, B., Yin, Y.: Enhanced effect and mechanism of SiO_2 addition in superhydrophilic property of TiO_2 films. Surf. Coat. Tech. **173**, 219–223 (2003)
28. Guan, K.: Relationship between photocatalytic activity, hydrophilicity and self-cleaning effect of TiO_2/SiO_2 films. Surf. Coat. Tech. **191**, 155–160 (2005)
29. Aberoomand Azar, P., MoradiDehaghi, Sh, Samadi, S., Saber Tehrani, M., Givianrad, M.H.: Effect of CMC and HPC mixture on the photocatalytic activity of Nd–TiO_2/SiO_2 film under visible light irradiation. Turk. J. Chem. **35**, 37–44 (2011)
30. Samadi, S.: Effect of HPC, PEG, CMC and PVP on the microstructure and photocatalytic activity of Nd–TiO_2/SiO_2 films under visible light irradiation. Asian J. Chem. **24**, 3649–3652 (2011)
31. Yaghoubi, H., Taghavinia, N., Keshavarz Alamdari, E.: Self cleaning TiO_2 self cleaning TiO_2 coating on polycarbonate: surface treatment photocatalytic and nanomechanical properties. Surf. Coat. Tech. **204**, 1562–1568 (2010)
32. Ye, X., Zhou, Y., Chen, J., Sun, Y.: Synthesis and infrared emissivity study of collagen-g-PMMA/Ag@TiO_2 composite. Mater. Chem. Phys. **106**, 447–451 (2007)
33. Gao, W., Chen, J., Guan, X., Jin, R., Zhang, F., Guan, N.: Catalytic reduction of nitrite ions in drinking water over Pd–Cu/TiO_2 bimetallic catalyst. Catal. Today **93–95**, 333–339 (2004)
34. Jiao, J., Xu, Q., Li, I.: Porous TiO_2/SiO_2 composite prepared using PEG as template direction reagent with assistance of supercritical CO_2. J. Colloid Inter. Sci. **316**, 596–603 (2007)

35. Zhao, G., Tian, Q., Liu, Q., Han, G.: Effects of HPC on the microstructure and hydrophilicity of sol–gel-derived TiO_2 films. Surf. Coat. Tech. **198**, 55–58 (2005)
36. Zheng, M.P., Gu, M.Y., Jin, Y.P., Wang, H.H., Zu, P.F., Tao, P., He, J.B.: Effects of PVP on structure of TiO_2 prepared by the sol–gel process. Mater. Sci. Eng., B **87**, 197–201 (2001)
37. Soler-Illia, G., Louis, A., Sanchez, C.: Synthesis and characterization of mesostructure titania-based materials through evaporation-induced self-assembly. Chem. Mater. **14**, 750–759 (2002)
38. Yu, J., Zhang, L., Zheng, Z., Zhao, J.: Synthesis and characterization of phosphate mesoporous titanium dioxide with high photocatalytic activity. Chem. Mater. **15**, 2280–2286 (2003)